Molecular Biology of the Cell
Vol. 17, 4093–4104, September 2006

A Global, Myosin Light Chain Kinase-dependent Increase in Myosin II Contractility Accompanies the Metaphase–Anaphase Transition in Sea Urchin Eggs[V]

Amy Lucero,* Christianna Stack,* Anne R. Bresnick,† and Charles B. Shuster*‡

*Department of Biology, New Mexico State University, Las Cruces, NM 88003; †Department of Biochemistry, Albert Einstein College of Medicine, Bronx, NY 10461; and ‡Marine Biological Laboratory, Woods Hole, MA 02543

Submitted February 9, 2006; Revised June 15, 2006; Accepted July 5, 2006
Monitoring Editor: Yu-li Wang

Myosin II is the force-generating motor for cytokinesis, and although it is accepted that myosin contractility is greatest at the cell equator, the temporal and spatial cues that direct equatorial contractility are not known. Dividing sea urchin eggs were placed under compression to study myosin II-based contractile dynamics, and cells manipulated in this manner underwent an abrupt, global increase in cortical contractility concomitant with the metaphase–anaphase transition, followed by a brief relaxation and the onset of furrowing. Prefurrow cortical contractility both preceded and was independent of astral microtubule elongation, suggesting that the initial activation of myosin II preceded cleavage plane specification. The initial rise in contractility required myosin light chain kinase but not Rho-kinase, but both signaling pathways were required for successful cytokinesis. Last, mobilization of intracellular calcium during metaphase induced a contractile response, suggesting that calcium transients may be partially responsible for the timing of this initial contractile event. Together, these findings suggest that myosin II-based contractility is initiated at the metaphase–anaphase transition by Ca^{2+}-dependent myosin light chain kinase (MLCK) activity and is maintained through cytokinesis by both MLCK- and Rho-dependent signaling. Moreover, the signals that initiate myosin II contractility respond to specific cell cycle transitions independently of the microtubule-dependent cleavage stimulus.

INTRODUCTION

At its most fundamental level, cytokinesis in animal cells is brought about by regional differences in cortical contractility that drives partitioning of the cytoplasm into two daughter cells (Wang, 2005). Force generation is accomplished by the transient assembly of a contractile ring, and recent genetic and proteomic approaches have significantly increased our knowledge of ring components and regulatory molecules (Echard *et al*., 2004; Eggert *et al*., 2004; Skop *et al*., 2004). Studies in yeast using green fluorescent protein-tagged ring components have demonstrated that ring components are recruited to the division site in a hierarchical manner that involves the progressive assembly of more complex structures (Lippincott and Li, 1998; Wu *et al*., 2003; Wu and Pollard, 2005). In contrast, the temporal sequence in which ring components are recruited to the division site in animal cells is not as well resolved; thus, it remains unclear whether the contractile ring assembles in a similar sequential manner. Moreover, it is not known how ring assembly is coordinated in space and time with chromosome segregation. Thus, although great advances have been made in our understanding of the contractile ring itself, fundamental gaps remain in our understanding of the spatiotemporal regulation of cytokinesis.

The mechanical nature of cytokinesis was appreciated by early cell biologists (Wilson, 1928; Rappaport, 1996), and for decades investigators have taken advantage of the large size and regular geometry of echinoderm eggs to study the biophysical changes in the cell surface during cell division. Using a variety of quantitative methods, changes in cortical tension were observed leading up to and during cytokinesis, but their timing relative to the nuclear division cycle or the physiological significance of these changes was unknown (Mitchison and Swann, 1955; Hiramoto, 1963, 1970, 1990; Yoneda and Dan, 1972; Yoneda *et al*., 1978; Yoneda and Schroeder, 1984; Yoneda, 1986). A common observation among many of these studies is a sharp, transient increase in cortical tension several minutes before furrow initiation (Yoneda and Dan, 1972; Usui and Yoneda, 1982; Ohtsubo and Hiramoto, 1985), which has been attributed to an increase in cortical actin (Usui and Yoneda, 1982). Simultaneous monitoring of polar and equatorial surfaces in sea urchin eggs (Ohtsubo and Hiramoto, 1985), and later in cultured mammalian cells, (Burton and Taylor, 1997; Matzke *et al*., 2001) revealed a dramatic but regionally restricted increase in tension at the cell equator. Although these physical changes were probably produced due to a balance between equatorial contractility and polar cortical tension (Robinson and Spudich, 2000; Girard *et al*., 2004; Reichl *et al*.,

This article was published online ahead of print in *MBC in Press* (http://www.molbiolcell.org/cgi/doi/10.1091/mbc.E06–02–0119) on July 12, 2006.

[V] The online version of this article contains supplemental material at *MBC Online* (http://www.molbiolcell.org).

Address correspondence to: Charles Shuster (cshuster@nmsu.edu).

Abbreviations used: CaFSW, calcium-free seawater; IP_3 inositol-1,4,5-triphosphate; MLCK, myosin light chain kinase; MRLC, myosin regulatory light chain; NEB, nuclear envelope breakdown; ROCK, Rho-kinase.

2005; Wang, 2005), the primary mediator of these physical changes is myosin II.

Myosin II is the force-generating motor for cytokinesis and is subject to regulation by both heavy and regulatory light chain phosphorylation (Matsumura *et al*., 2001; Matsumura, 2005). Our understanding of heavy chain phosphorylation comes primarily from studies on the slime mold *Dictyostelium discoideum*, where phosphorylation of the tail region by a family of heavy chain kinases inhibits filament formation (Egelhoff *et al*., 1993; Sabry *et al*., 1997; Yumura and Uyeda, 1997; Zang and Spudich, 1998; Yumura *et al*., 2005). The expression of nonphosphorylatable heavy chain mutants results in abnormally high myosin II recruitment to the cell equator, whereas expression of myosin II heavy chains containing amino acid substitutions that mimic the phosphorylated state prevents recruitment to the contractile ring (Sabry *et al*., 1997; Yumura, 2001). These phosphorylation sites reside in a C-terminal extension of myosin heavy chain that is required for proper cytokinesis in *Dictyostelium* (O'Halloran and Spudich, 1990) but is absent from myosin II in animal cells. In mammalian cells, protein kinase C and casein kinase II phosphorylate myosin II heavy chain (Murakami *et al*., 1998, 2000; Bresnick, 1999; Dulyaninova *et al*., 2005), and the S100 family protein metastasin 1 binds to and prevents myosin IIA filament assembly (Li *et al*., 2003). However, the functional significance of the regulatory mechanisms during cell division remains unclear.

Phosphorylation of the myosin regulatory light chain (MRLC) both positively and negatively regulates myosin II, and both mechanisms have been implicated in regulating myosin II during cytokinesis (Satterwhite *et al*., 1992; Bresnick, 1999; Matsumura, 2005). Light chain phosphorylation on Ser19 and Thr18 activates myosin by promoting both myosin/actin interactions and filament assembly (Scholey *et al*., 1980; Ikebe *et al*., 1988) and nonphosphorylatable mutants of MRLC block cytokinesis in *Drosophila* and mammalian cells (Jordan and Karess, 1997; Simerly *et al*., 1998; Komatsu *et al*., 2000). Multiple kinases have been implicated in mediating MRLC phosphorylation on these sites, either by directly phosphorylating Ser19 or by inhibiting myosin phosphatase (Matsumura, 2005). Although the Ca^{2+}/calmodulin-dependent myosin light chain kinase (MLCK) and Rho-kinase (ROCK) are likely candidates, genetic or chemical inhibition studies have implicated only citron kinase, and it seems to function late in cytokinesis (Echard *et al*., 2004; Naim *et al*., 2004). Therefore, the kinase or kinases mediating myosin light chain phosphorylation early in cytokinesis have not been fully elucidated.

To examine the timing of myosin II contractility in living cells as well as dissect the signals that influence myosin II activation, we have developed a compression assay that detects subtle changes in the isotropic cytoskeleton of sea urchin eggs (Stack *et al*., 2006). We report here that myosin II is transiently and globally activated before cleavage plane specification. Moreover, myosin II activation during cell division requires multiple inputs from different signaling pathways, giving rise to a model whereby calcium-dependent signaling mediates the global activation of myosin, and Rho-dependent signaling focuses on contractility for cytokinesis.

MATERIALS AND METHODS

Embryo Culture

The sea urchin *Lytechinus pictus* was used for all the experiments in this study. *Lytechinus pictus* were obtained from Marinus (Long Beach, CA) and maintained in artificial seawater at 15°C. Gametes were obtained by intracoelemic injection of 0.5 M KCl. A 1:1000 dilution of sperm was added to a 5% egg suspension, and eggs were gently pelleted by hand centrifugation and resuspended in Ca^{2+}-free seawater (CaFSW). Fertilization envelopes were removed by passing the eggs through 150-μm Nitex three times, and zygotes were cultured in CaFSW at 15°C until needed. To generate eggs with supernumerary asters, cells were treated with hypertonic seawater as described previously (Sluder *et al*., 1997). Briefly, at 10 min after fertilization, eggs were washed with hypertonic CaFSW (8 ml of 2.5 M NaCl added to 50 ml CaFSW, pH 8.9) for 15 min and then washed back with isotonic CaFSW.

Chemicals and Reagents

Unless noted otherwise, all chemicals were purchased from Sigma-Aldrich (St. Louis, MO). Blebbistatin, nocodazole, ML-7, and H-1152 were purchased from Calbiochem (San Diego, CA). Rho-guanine nucleotide dissociation inhibitor (Rho-GDI) was purchased from Cytoskeleton (Denver, CO), and P4(5)-(1-(2-nitrophenyl)-ethyl) ester (NPE)-caged inositol-(1,4,5)-trisphosphate (cIP_3) and calcium-green dextran (mol. wt. 10,000) were purchased from Invitrogen (Carlsbad, CA). The antennapedia-MLCK inhibitory peptide (RQIKIWFQNRRMKWKK AKKLSKDRMKKYMARRKWQKTG) was synthesized at the Tufts University Core Facility (Boston, MA).

Micromanipulation

To observe changes in cortical contractility during the cell cycle, eggs were placed under compression using a gas-permeable fluorocarbon oil (Sluder *et al*., 1999; Stack *et al*., 2006). Briefly, fertilized eggs stripped of their fertilization envelopes were placed in a glass-bottomed 35-mm culture dish (WPI, Sarasota, FL) precoated with 10 mg/ml protamine sulfate (Sigma-Aldrich) and allowed to settle for 5 min. The eggs were compressed 40 min after fertilization by rapidly removing seawater and replacing with 1.5 ml of Fluorinert FC-40 oil (Sigma-Aldrich). Measurements of cell geometry were performed using ImageJ (http://rsb.info.nih.gov/ij/).

Microinjection

All reagents for microinjection were resuspended in injection buffer (10 mM HEPES and 150 mM sodium aspartate, pH 7.0) and back-filled into glass capillary pipettes (WPI). In all injection experiments, cells were injected with ~10–40 pl (1.4–5.7% of cell volume) before withdrawal of seawater and replacement of FC-40 oil.

To visualize chromosome segregation in living sea urchin embryos, eggs were microinjected at the single-cell stage shortly after fertilization with 1 mg/ml calf histone labeled with Alexa Fluor-488 (Protein Labeling kit; Invitrogen). For calcium mobilization experiments, eggs were microinjected with 2 mM calcium green dextran and 2 mM NPE-cIP_3 under safelight conditions 10–15 min after fertilization. Injected eggs were then compressed under Fluorinert FC-40 oil ~10 min after microinjection and observed by differential interference contrast (DIC)/ fluorescein isothiocyanate (FITC) fluorescence at 10-s intervals through nuclear envelope breakdown, after which cells received a single 500-ms pulse of UV light to uncage the IP_3 and mobilize intracellular calcium.

Detection of Ser19 Phosphorylation In Vivo

Lytechinus pictus eggs were fertilized, stripped of their fertilization envelopes and cultured up until the first mitosis. Cells were then fixed and permeablized using a protocol optimized for visualizing the actin cytoskeleton (Wong *et al*., 1997). Cells were then washed, blocked with 3% bovine serum albumin in phosphate-buffered saline/2 mM NaF, and processed for tubulin (DM1A; Sigma-Aldrich), activated myosin II [rabbit or mouse anti-phospho(Ser19)-myosin regulatory light chain; Cell Signaling Technology, Beverly, MA], or egg myosin II localization. Primary antibodies were detected with Alexa Fluor-labeled secondary antibodies (Invitrogen), and confocal images were acquired using an Olympus FluoView confocal microscope (Olympus America, Melville, NY) at the Central Microscopy Facility at the Marine Biological Laboratory (Woods Hole, MA).

Imaging Acquisition and Processing

All live cell experiments were performed on Zeiss Axiovert 200M microscopes equipped with computer-driven Uniblitz (Vincent Associates, Toronto, Ontario, Canada) and internal fluorescence shutters to control bright field and epifluorescence light sources. Brook Industries (Lake Villa, IL) heating/cooling stage inserts were used to maintain sample temperature at 15°C. DIC and fluorescence images were recorded using a 12-bit Axiocam charge-coupled device (CCD) camera driven by AxioVision 4.2, and figures were prepared using ImageJ version 1.34, Adobe Photoshop 6.0.1 (Adobe Systems, Mountain View, CA), and QuickTime software (Apple Computer, Cuptertino, CA). For polarization microscopy, an Axiovert 200M was configured with a circular polarizer and 546-nm filter placed above the condenser, and a liquid crystal universal compensator (LC-Polscope; Cambridge Research Instruments, Woburn, MA) was placed below the reflector turret (Oldenbourg and Mei, 1995). An EXFO X-Cite 120 light source (Exfo Life Sciences, Mississauga, Ontario, Canada) was used for transillumination, and images were acquired using a Q Imaging cooled CCD camera controlled by PSJ software (Marine

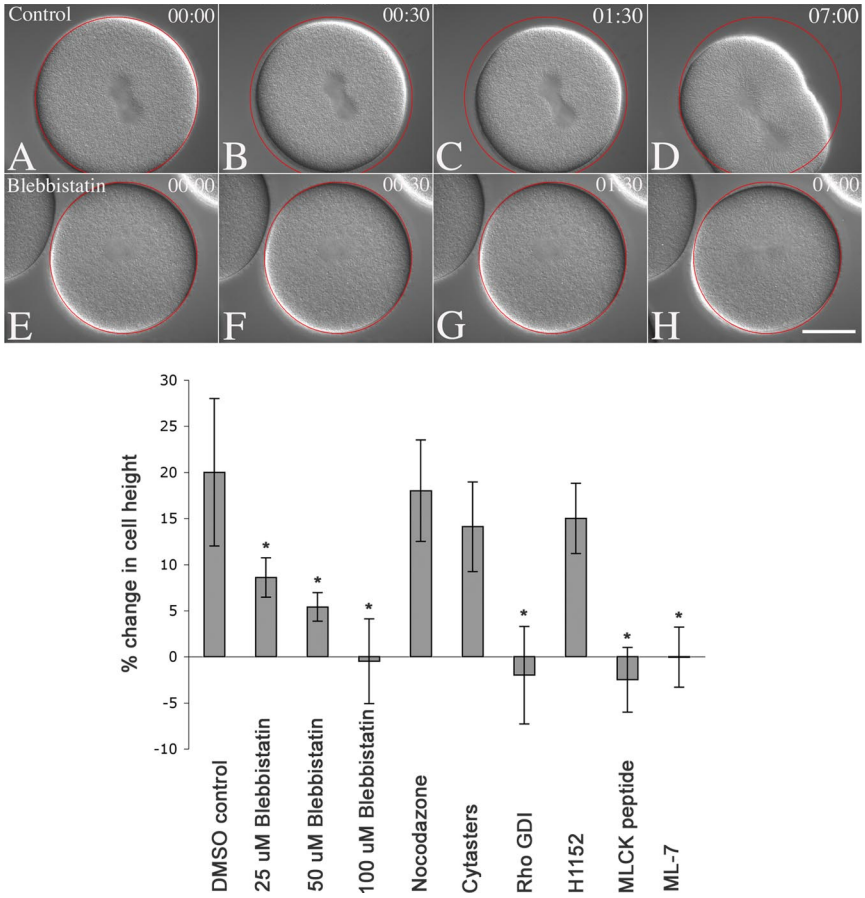

Figure 1. Detection of changes in cortical contractility in flattened sea urchin eggs. Top, *L. pictus* eggs were fertilized, compressed under fluorocarbon oil, and followed by time-lapse microscopy, with each series beginning just before the metaphase–anaphase transition. In control cells (A–D), there was a sharp decrease in cell diameter, followed by a brief relaxation and appearance of the cleavage furrow. Blebbistatin (50 μM; E–H) suppressed both the initial increase in contractility as well as furrow ingression. The red circle denotes the cell boundary at metaphase. Bar, 50 μm. Bottom, increases in cortical tension result in an increase in cell height as resistance to compression increases. For each condition described, cell height was calculated 30 s before and 180 s after the metaphase–anaphase transition, and the contractile response is expressed as a percentage of change in cell height. Error bars reflect SD, and asterisks indicate significances of $p \leq 0.007$.

Biological Laboratory). Image stacks were acquired using a 3-nm retardance ceiling, exported as 8-bit tiffs to ImageJ, where kymographs as well as three-dimensional surface projections were generated. Figures were prepared with Adobe Photoshop 6.0.

RESULTS

A Global Increase in Cortical Contractility Accompanies the Metaphase–Anaphase Transition

Classic studies on the biophysical properties of the cell surface by Hiramoto and others have demonstrated that in many echinoderm species, there is an increase in cortical "stiffness" before cytokinesis (Hiramoto, 1990; Rappaport, 1996). Other studies in sea urchin eggs suggested that the acquisition of furrow-inducing capacity or cortical responsiveness occurs abruptly at the metaphase–anaphase transition (Shuster and Burgess, 2002b), and we sought to develop a physical manipulation that would detect early events leading up to cytokinesis. A classical method for studying changes in cortical contractility in echinoderm eggs has been to measure resistance to compression (Cole, 1932; Cole and Michaelis, 1932; Yoneda, 1964; Yoneda, 1986). More recently, we found that a common method for observing mitosis in sea urchin eggs (Sluder *et al*., 1999) provided a sensitive and convenient microscopic assay for detecting myosin II-dependent, blebbistatin-sensitive changes in cortical contractility during fertilization (Stack *et al*., 2006). As shown in Figure 1, sea urchin blastomeres plated onto glass-bottomed culture dishes could be flattened from a diameter of ~110 μm to a thickness of 18–30 μm by rapidly exchanging seawater with a gas-permeable fluorocarbon oil. Cells flattened in this manner remained viable for up to 8 h and continued to divide, although extremely flat cells frequently failed to complete cytokinesis. Cells manipulated in this manner were followed through the first cell cycle in the absence (Figure 1, A–D, top) or presence of 50 μM blebbistatin (Figure 1, E–H, top), an inhibitor of nonmuscle myosin II ATPase activity (Straight *et al*., 2003; Kovacs *et al*., 2004) that also blocks myosin contractility in cytokinesis in sea urchin eggs (Ng *et al*., 2005; Stack *et al*., 2006). As shown in Figure 1, A–D (and Supplemental Videos 1 and 6), in control cells there was a sharp increase in cortical tension ~13 min after nuclear envelope breakdown (NEB), as evidenced by the decrease in cell diameter as the cell resisted compression (Figure 1B). The initial increase in cortical contractility was followed by a brief relaxation before the onset of furrowing (Figure 1D). The amplitude of this prefurrow "contraction" was roughly proportional to the degree of flattening, with less pronounced contractions seen in cells flattened to a thickness of $\geq$30 or $<$17 μm. However, in each case ($n = 45$), a cortical contraction preceded the onset of furrowing. In contrast, blebbistatin suppressed both the initial increase in contractility, and the cleavage furrow in a dose-dependent manner (Figure 1, bottom), suggesting that the increased resistance to compression was dependent on myosin II (Figure 1, E–H, and Supplemental Video 2). Although off-target effects have been reported (Shu *et al*., 2005), blebbistatin was effective at concentrations between 25 and 100 μM (Figure 1, bottom) without affecting F-actin assembly and organization, cortical granule release, or calcium signaling (Stack *et al*., 2006).

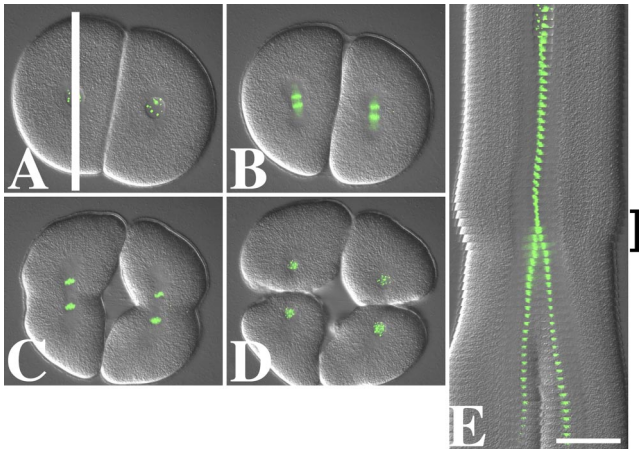

Figure 2. Prefurrow cortical contractility initiates at the metaphase–anaphase transition. *Lytechinus pictus* eggs were injected at the single-cell stage with Alexa Fluor-488–labeled histone to label chromatin (shown in green). After the first cell division, cells were flattened under FC-40 oil, and fluorescence/DIC images were taken every 30 s through the second division (A–D). The white bar in A denotes the slice removed from the image stack to create the kymograph in E. The onset of contractility (denoted by the bracket) preceded the onset of sister chromatid segregation by 60 s. Bar, 50 μm.

The sudden onset of cortical contractility in flattened sea urchin eggs seemed to coincide with the metaphase–anaphase transition, which also coincided with the earliest onset of furrow-inducing activity measured in cylindrical cells (Shuster and Burgess, 2002b). To better visualize chromosome segregation in cells under compression, fertilized eggs were injected with fluorescently labeled histone before flattening and nuclear envelope breakdown, and followed through the first and second cell divisions (Figure 2 and Supplemental Video 3). Simultaneous imaging of chromosome segregation and contractility revealed that in each case (n = 9), contractility initiated ~60 s before the first visible poleward chromatid movements (Figure 2E, bracket). Thus, the ability to unambiguously follow cortical contractility relative to the nuclear clock allowed us to assign the onset of myosin II contractility to the metaphase–anaphase transition.

Live cell imaging of dividing cells revealed a transient increase in cortical contractility coincident with the metaphase–anaphase transition (Figures 1 and 2). Previous mapping of MRLC phosphorylation in dividing sea urchin eggs revealed an increase in cortical Ser19 phosphorylation during anaphase but detected little Ser19 phosphorylation during metaphase (Shuster and Burgess, 1999). To examine myosin activation in vivo, fertilized eggs were fixed and processed for microtubule and phospho-Ser19 MRLC localization (Figure 3) by using an antibody previously demonstrated to react with phosphorylated sea urchin myosin regulatory light chain (Stack *et al*., 2006). Roughly half (30/55 cells scored) of the cells in metaphase (75 min after fixation) had a bright cortical rim of Ser19 phosphorylation (Figure 3, A–F). This contrasted sharply with cells in an-

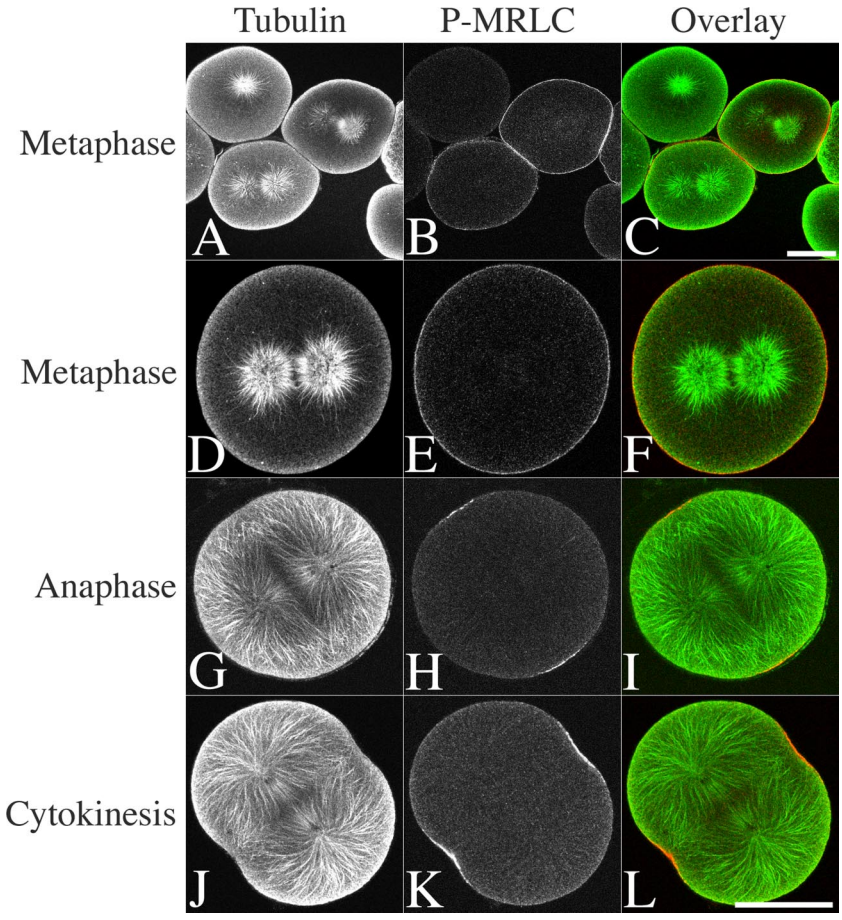

Figure 3. Localization of myosin regulatory light chain phosphorylation in dividing sea urchin eggs. *Lytechinus pictus* eggs were fertilized, stripped of their fertilization envelopes, and fixed at intervals through the first cell division. Eggs were permeablized and processed for α-tubulin (A, D, G, and J) and phospho-Ser19 MRLC (B, E, H, and K) localization and imaged by confocal microscopy. In the low magnification image shown in A–C (bar, 50 μm), approximately half of cells fixed late in metaphase had detectable phosphorylated regulatory light chain in the cortex. In contrast to metaphase cells (A–F), cells in anaphase with elongated astral microtubules had little light chain phosphorylation in the cortex except at the equator (G–I). By the onset of furrowing (J–L), phosphorylated light chain was concentrated in a broad band at the equator. Bar, 50 μm.

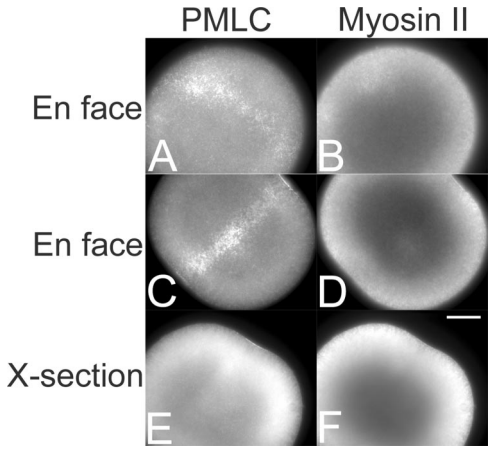

Figure 4. Enrichment of Ser19-phosphorylated myosin light chain at the cell equator. Fertilized *L. pictus* eggs were fixed after anaphase onset and processed for PMLC (A, C, and E) and nonmuscle myosin II (B, D, and F) localization and then imaged by wide-field fluorescence microscopy. Cells imaged en face (A–D) or in cross section (E and F) displayed an equatorial accumulation of phosphorylated myosin light chain, but no overall enrichment of myosin II. Bar, 25 μm.

aphase or cytokinesis, where light chain phosphorylation was confined to the cleavage plane (Figure 3, G–L). Although the level of cell synchrony was not sufficient to resolve early versus late metaphase (Figure 3, A–C), the presence of activating myosin II phosphorylation in the cortex of cells with aligned chromosomes (our unpublished data) and a well-developed mitotic apparatus supported our findings in living cells that there was an increase in contractility at the metaphase–anaphase transition (Figures 1 and 2).

The observed changes in Ser19-phosphorylated MRLC distribution during anaphase (Figure 3) could reflect differences in either the activation state of myosin II or its enrichment in the cortical cytoskeleton. To determine whether the equatorial band of Ser19-phosphorylated MRLC reflected local changes in myosin II activation or recruitment, dividing cells were stained for Ser19-phosphorylated MRLC and total myosin, and imaged by wide-field fluorescence microscopy (Figure 4). En face views of the cell surface (Figure 4, A–D) revealed a 13 ± 2.2-μm zone of phosphorylated MRLC that was visible in anaphase eggs (Figure 4, A and B) as well as actively cleaving eggs in the cylinder stage (Figure 4, C–F). In contrast, staining with antibodies against egg myosin II (Figure 4, B, D, and F) or fluorescent phalloidin (our unpublished data) revealed a uniform distribution of myosin II and F-actin throughout the cortex with very little detectable enrichment at the cell equator, suggesting that in these early stages of cytokinesis, the equatorial band of Ser19 phosphorylated MRLC was due to local changes in myosin II activation.

Global Activation of Myosin Precedes Cleavage Plane Specification

Multiple roles have been proposed for microtubules in cleavage plane determination (Rappaport, 1996; Burgess and Chang, 2005), and there is now general agreement that microtubules are required for cleavage plane determination as well as the maintenance of the cleavage furrow and abscission (Wheatley and Wang, 1996; Larkin and Danilchik, 1999). Although the molecular nature of the cleavage stimulus remains unknown, recent studies in sea urchin eggs demonstrated a microtubule-dependent localization of active Rho GTPase at the cleavage plane before furrow initiation (Bement *et al*., 2005). The increase of cortical contractility at anaphase onset (Figures 1 and 2) seemed to precede cleavage plane determination, which normally occurs 1 min after contact between the cortex and the astral arrays (Rappaport and Ebstein, 1965) or ~7 min after anaphase onset in *L. pictus* eggs (Shuster and Burgess, 2002b). To examine the timing of myosin II activation relative to cleavage plane determination, spherical and flattened eggs were followed using liquid crystal polarization microscopy (Oldenbourg and Mei, 1995). In the unflattened cell shown in Figure 5, A–D, a sharp drop in spindle birefringence was detected within 30 s after anaphase onset, as astral microtubules elongate and

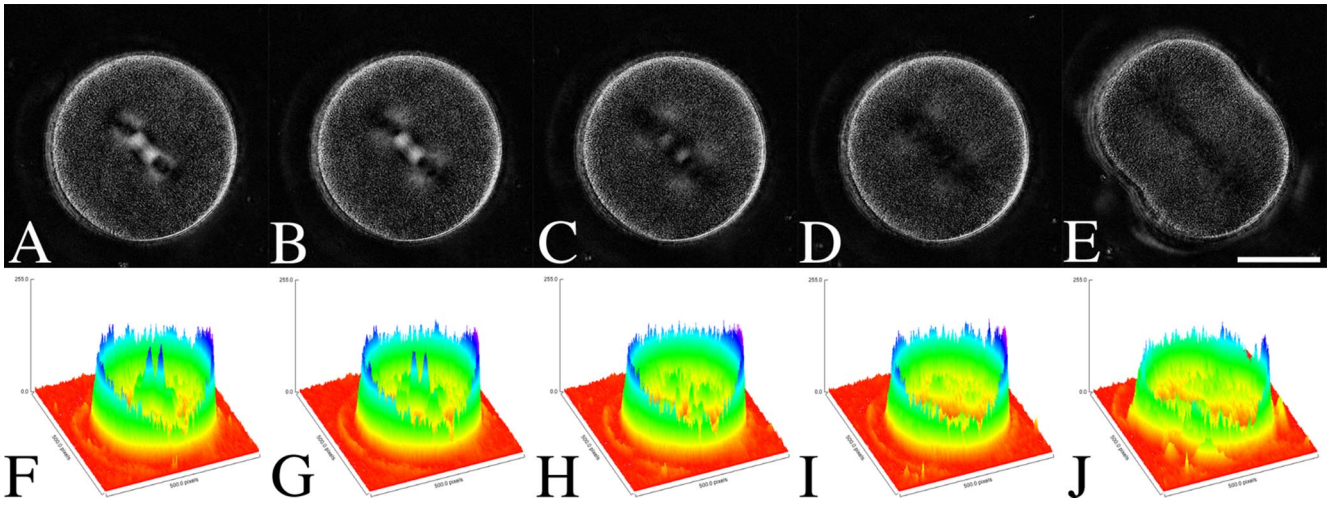

Figure 5. Changes in spindle birefringence leading up to furrow formation in spherical sea urchin eggs. *Lytechinus pictus* eggs were fertilized, stripped of their fertilization membranes, and followed by orientation-independent polarization microscopy (A–E). At anaphase onset (B), spindle birefringence drops rapidly as the kinetochore fibers disappear and the astral microtubules extend out to the cortex (C–E). F–J illustrates the drop in spindle birefringence (shown as four peaks in the center) relative to edge birefringence by using surface plots derived from the images shown in A–E, respectively. Bar, 50 μm.

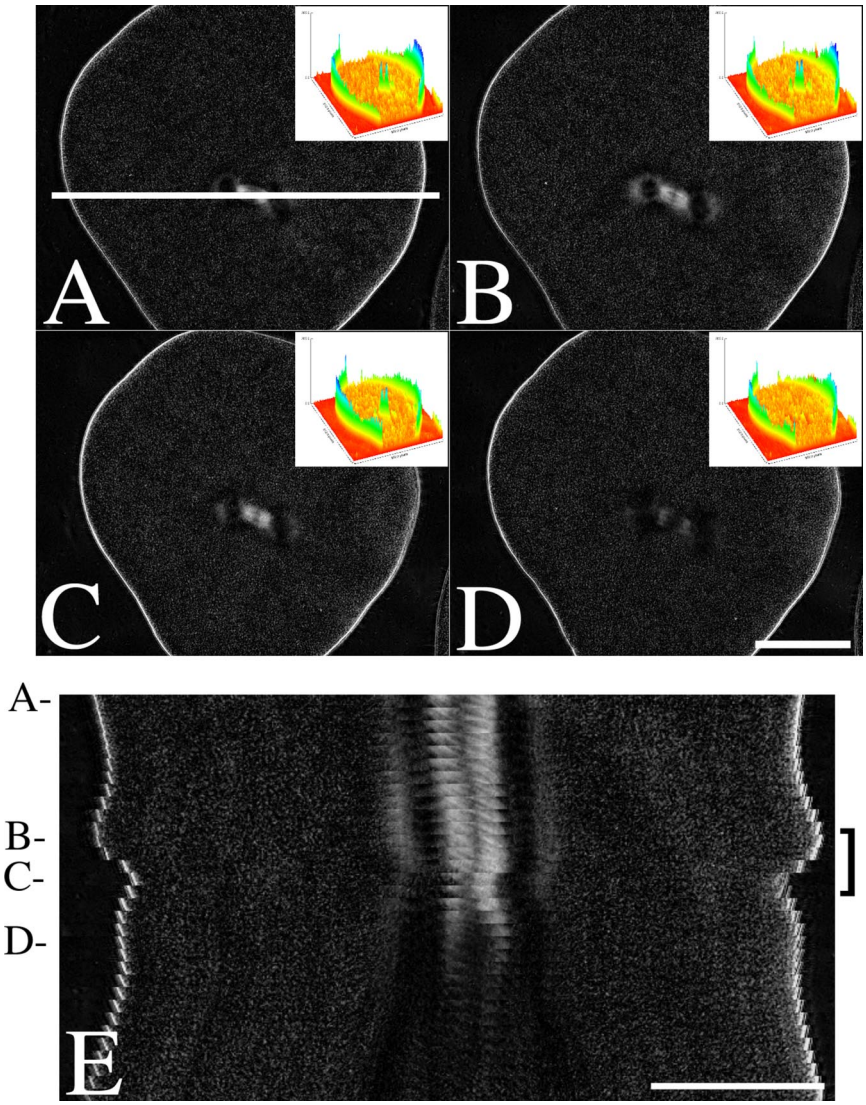

Figure 6. Increase in cortical contractility precedes the shift in spindle birefringence and elongation of the asters. *Lytechinus pictus* eggs were fertilized, stripped of their fertilization membranes, and flattened shortly before NEB. Cells were followed by orientation-independent polarization microscopy (A–E), and a slice was cropped from each image in the stack (denoted by the white bar in A) to generate the kymograph in E. Note the transient global contraction (brackets) precedes the drop in spindle birefringence. A–D represent frames 1, 12, 15, and 20, respectively. Bar, 50 μm.

contact the cell cortex. Approximately 7 min after anaphase onset, the first detectable surface activity was observed at the cell equator (Figure 5, C and D, Supplemental Video 4). When flattened cells were examined (Figure 6 and Supplemental Video 5), ingression of the cell margin preceded the transition in microtubule dynamics by 60 s (Figure 6E). This was visible both in the raw image as well as in a surface plot of retardance values (Figure 6, insets, and Supplemental Video 5), where the ingression of the cell margins clearly preceded the drop in spindle birefringence. Although the increase in cortical contractility was closely tied to anaphase onset, it appeared that the increase in myosin II contractility preceded the stabilization of microtubule dynamics and cleavage plane determination.

The well-documented shift in microtubule dynamics that accompanies mitotic exit in sea urchin eggs lagged slightly behind the increase in cortical contractility (Figure 6), supporting the localization studies (Figure 3) suggesting that the initial activation of myosin II precedes the positioning and assembly of the contractile ring. Several lines of experimentation have suggested that high concentrations of microtubules suppress actomyosin contractility (Canman and Bement, 1997) and that the localization of the contractile ring arises from a local deficit of microtubules at the equatorial plane (Schroeder, 1972; Dechant and Glotzer, 2003). To further explore any possible role that microtubules might play in regulating cortical contractility, cells were treated before metaphase with reagents that modulate microtubule dynamics or density (Figure 7). To reduce microtubule polymer in cells, cells were treated with 50 μM nocodazole (Figure 7B) to prevent spindle assembly. Although reduction or depolymerization of the mitotic apparatus can delay anaphase and mitotic exit in sea urchin eggs (Sluder, 1976, 1979), nocodazole did not significantly suppress the increase in myosin II contractility (Figures 1, bottom, and 7B′, and Supplemental Video 7); however, the subsequent relaxation observed in control cells did not occur in nocodazole treated cells (n = 10) (compare Figures 7A′ and 6B′, respectively). To examine whether astral microtubule–cortex interactions could suppress prefurrow contractility, fertilized eggs were treated briefly with hypertonic seawater, which results in de novo centriole formation (Kuriyama and Borisy, 1983; Kallenbach, 1985; Sluder *et al*., 1997). As shown in Figure 7, C and C′ (and Supplemental Video 8), as many as 35 supernumery asters (or cytasters) appeared at the onset of mitosis. The presence of microtubule asters throughout the cyto-

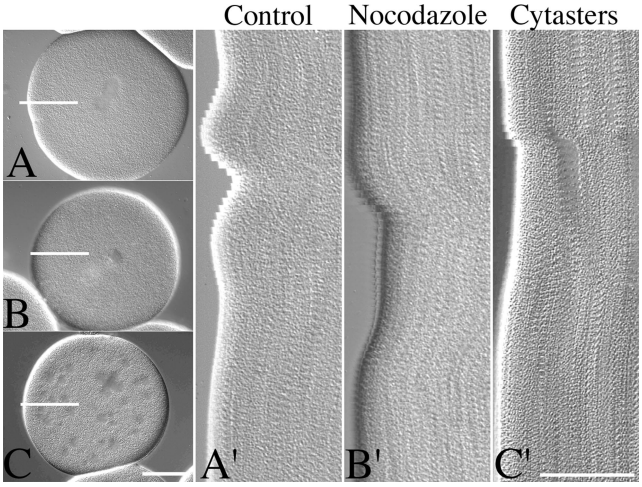

Figure 7. Microtubules do not influence myosin II activation. *Lytechinus pictus* eggs were fertilized and cultured in 0.1% dimethyl sulfoxide (DMSO) (A and A′), 50 μM nocodazole (B and B′) to depolymerize the mitotic spindle, or supernumery asters (cytasters) were induced by brief treatment with hypertonic seawater (C and C′). Eggs were flattened and followed by DIC time-lapse microscopy with images acquired every 30 s. Kymographs (A′–C′) were generated from image slices cropped from the image stack (denoted by white bars). Bar, 50 μm (C) and 25 μm (C′).

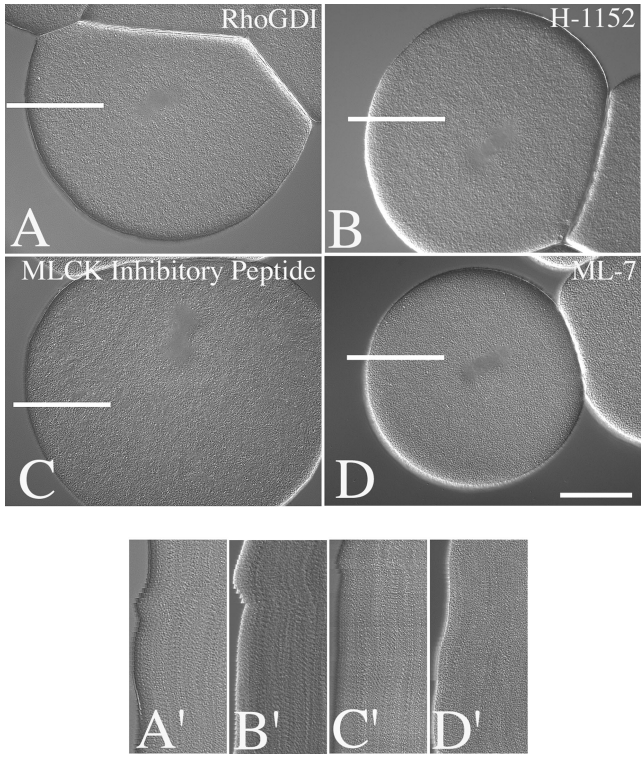

Figure 8. Initiation of myosin II contractility is dependent on MLCK. *Lytechinus pictus* eggs were injected with 3 mg/ml Rho-GDI (A and A′) or treated with 1 μM H-1152 (B and B′) to suppress Rho GTPase or ROCK activity, respectively. To inhibit MLCK activity, cells were injected with 4 mg/ml MLCK inhibitory peptide (C and C′) or treated with 50 μM ML-7 (D and D′) before flattening. Images were acquired every 30 s, and image slices were cropped from the image stack (denoted by white bars) to generate kymographs in A′–D′. Bar, 50 μm.

plasm failed to suppress prefurrow contractility; however, the amplitude of the contractile response was slightly dampened relative to controls (Figures 1, bottom, and 7A, and Supplemental Movie 6). Thus, the activation of prefurrow cortical contractility appeared to be independent of microtubules, but the transient relaxation before furrow formation was sensitive to microtubule depletion.

Roles of MLCK and ROCK on Myosin II Activation

Studies of live and fixed sea urchin eggs suggested that the onset of contractility occurred at the metaphase–anaphase transition (Figures 2–5). These data fit earlier predictions suggesting that the proximal signals for cytokinesis are triggered at the metaphase–anaphase transition (Shuster and Burgess, 1999, 2002b). As mentioned, MLCK, ROCK, and citron kinases have been implicated in the regulation of myosin II during cytokinesis (Matsumura *et al*., 2001, 2005), but citron kinase has been shown to act primarily at the end of cytokinesis. To identify the signaling pathways responsible for myosin II activation at the metaphase–anaphase transition, cells were treated or microinjected with reagents that inhibit either the Rho- or Ca^{2+}/MLCK signaling pathways (Figures 1, bottom, and 8). Microinjection of Rho-GDI, which binds GDP-Rho and inhibits exchange of GDP for GTP, resulted in a nearly complete loss of cortical tension (n = 7), with cells unable to resist compression (Figure 8, A and A′, and Supplemental Video 9). Similar results were observed with C3 transferase another Rho inhibitor (our unpublished data). However, a small, but detectable increase in contractile activity was detected at anaphase onset (Figure 8, A and A′). In cells treated with the ROCK inhibitor H-1152, the timing of nuclear envelope breakdown, metaphase–anaphase transition and prefurrow contractility was not significantly affected (Figure 1, bottom), although furrowing was inhibited (n = 26) (Figure 8, B and B′, and Supplemental Video 10).

To block MLCK function without compromising other calmodulin-dependent activities, cells were injected with an MLCK inhibitory peptide (Figure 8, C and C′, and Supplemental Video 11) that acts as a pseudosubstrate for MLCK (Kargacin *et al*., 1990) or were treated with ML-7 (Figure 8, D and D′, and Supplemental Movie 12). Complete inhibition of prefurrow contractility was observed with both the peptide and small molecule inhibitors (n = 8 and 7, respectively) (Figures 1, bottom, and 8, C′ and D′). These results suggested that the initial increase in cortical contractility was a MLCK-dependent but not ROCK-dependent process.

Rho GTPase is thought to direct contractile ring assembly, via the regulation of formins and myosin II contractility (Piekny *et al*., 2005). However, our data indicate that ROCK was not required for prefurrow myosin II activity (Figure 8). Additionally, the role of MLCK during cytokinesis as well as the relevance of global contractile events remains unclear. Therefore, to confirm that these signaling pathways are essential for cytokinesis in sea urchin eggs, unflattened cells were treated with H-1152 or ML-7 and subsequently scored for cleavage (n = 33 for each condition). Both ROCK- and MLCK-inhibited cells failed to complete cytokinesis as indicated by the binucleated cells in Figure 9, suggesting that both ROCK and MLCK signaling are necessary for proper cytokinesis in this cell type.

Precocious Activation of Cortical Tension during Cell Division

The Ca^{++}/calmodulin-dependent MLCK was required for the early activation of myosin II at the metaphase–anaphase

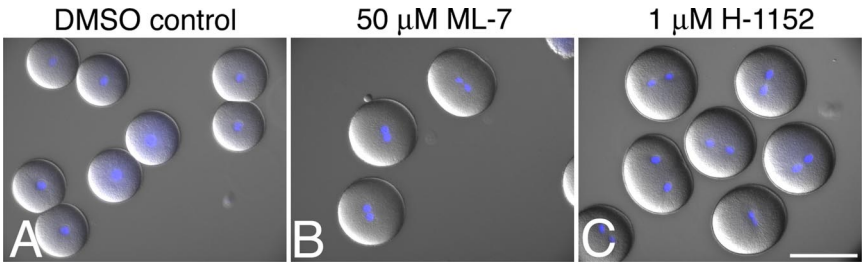

Figure 9. MLCK and ROCK are both required for proper cytokinesis in sea urchin eggs. Fertilized eggs were incubated in CaFSW for 60 min after fertilization and then transferred into CaFSW containing 0.1% DMSO (A), 50 μM ML-7 (B), or 1 μM H-1152 (C). Hoescht 33342 was added to 1 μg/ml before imaging to detect nuclear divisions (Blue). Note that although carrier control cells underwent normal nuclear and cytoplasmic divisions (A), cells with compromised MLCK (B) or ROCK (C) activity failed to undergo cytokinesis. Bar, 100 μm.

transition and also for the completion of cytokinesis (Figures 7 and 8). Calcium has been shown to be required for cytokinesis in several embryonic cell types (Fluck *et al*., 1991; Miller *et al*., 1993; Chang and Meng, 1995; Muto *et al*., 1996; Webb *et al*., 1997; Saul *et al*., 2004; Wong *et al*., 2005), and myosin activation (Shuster and Burgess, 2002a; Stack *et al*., 2006) as well as membrane addition (Shuster and Burgess, 2002a) are candidate downstream effectors. Imaging of calcium dynamics in dividing *L. pictus* eggs revealed that there is a mobilization of calcium at the metaphase–anaphase transition that is necessary for cytokinesis (Groigno and Whitaker, 1998), raising the possibility that this calcium transient may partially serve as the "timer" for the activation of myosin II. Thus, to establish whether calcium acts as an early signal for myosin II activation, fertilized eggs were injected with calcium green dextran and cIP_3 before flattening. cIP_3 was uncaged with a single pulse of UV light 3 min after NEB, when the cell was in early metaphase, and the calcium transient were detected by an increase in calcium green fluorescence. Uncaging of cIP_3 resulted in a detectable contractile response within one minute of the UV light pulse (Figure 10, bracket, and Supplemental Video 13) (n = 6), whereas exposure to UV light in the absence of cIP_3 induced no contractile response (Stack *et al*., 2006). Thus, even though the cell was in metaphase, at a time when myosin contractility is thought to be suppressed (Satterwhite *et al*., 1992), precocious mobilization of calcium was sufficient to induce a cortical contractile response.

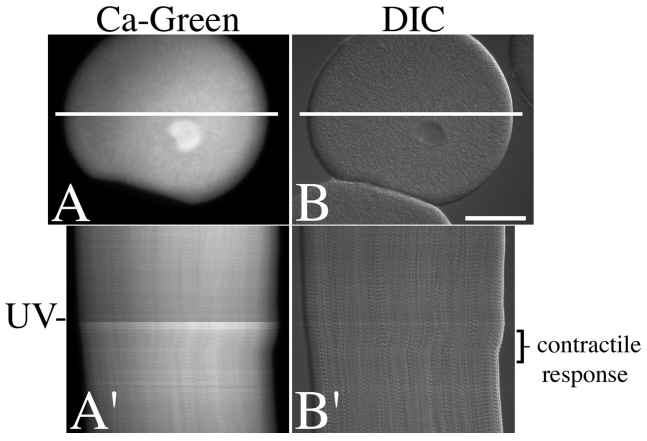

Figure 10. Mobilization of intracellular calcium induces cortical contractility in mitotic cells. *Lytechinus pictus* eggs were fertilized and injected with calcium green dextran and cIP_3 before compression under FC-40 oil. Cells were observed by FITC fluorescence (A and A′) and DIC (B and B′) microscopy, with images acquired every 10 s. Shortly after NEB, cells received a single pulse of UV light to uncage IP_3 and mobilize intracellular calcium. Kymographs (A′ and B′) were generated by cropping a slice from each image stack (A and B, white bars). The increase in calcium could be seen after the UV flash (UV left column) as in increase in calcium green fluorescence, and the contractile response (B′, bracket) could be detected within 30 s of calcium mobilization. Bar, 50 μm.

DISCUSSION

In animal cells, cytokinesis is a series of interrelated events that combine to partition the cytoplasm around the reforming daughter nuclei. These events include cleavage plane determination (by the mitotic apparatus), actin ring assembly, myosin II activation, ring constriction, ring disassembly, membrane addition, and midbody formation/abscission. In yeast, these events proceed in a sequential manner, with specific components being recruited to the bud neck/actin ring, and constriction and membrane addition occurring late in the process (Lippincott and Li, 1998; Wu *et al*., 2003; Wu and Pollard, 2005). Although the late events of cytokinesis seem to be well resolved, the sequence of early events leading to ring assembly in animal cells remains unclear. In an effort to address these issues, a simple yet sensitive manipulation of living cells was used to resolve the temporal and spatial dynamics of myosin II activation. The global activation of myosin II detected at the metaphase–anaphase transition is consistent with both the early biophysical studies of cytokinesis (Hiramoto, 1990; Rappaport, 1996) as well as more recent studies defining the earliest window of furrowing capacity (Rappaport and Rappaport, 1993; Shuster and Burgess, 2002b). Moreover, a recent study that measured forces at the surface of dividing sea urchin eggs reported a sharp increase in cortical tension 6 min before furrow initiation (Miyoshi *et al*., 2006). This initial increase in tension was isotropic and transient, with cortical tension rising again just before the onset of furrowing and oriented in the plane of the contractile ring. Force production by these "prefurrow spikes" ranged between 1.5 and 3 nN/μm for the three species tested (*Clypeaster japonicus*, *Hemicentrotus pulchrerrimus*, and *Scaphechinus mirabilis*). Although the compression method described here does not quantify changes in cortical tension, it allows for a more accurate measurement of the temporal coordination between chromosome segregation and prefurrow contractility (Figure 2). Lastly, these two independent methods (needle deflection and compression) demonstrate that cortical contractile activity is dependent on myosin II and MLCK. Thus, these studies shed novel insight not only into the molecular mechanisms contributing to myosin II activation but also the order of events leading up to the establishment and ingression of the cleavage furrow.

Myosin II Activation Precedes Cleavage Plane Determination

Recent studies in sea urchin eggs demonstrated that before furrow ingression, a zone of active Rho GTPase (Bement *et*

al., 2005) as well as a lipid raft markers (Ng *et al*., 2005) accumulate at the cell equator in a microtubule-dependent manner, but otherwise the sequence of early events leading to contractile ring formation is poorly resolved in animal cells. In sea urchin eggs, anaphase onset is accompanied by a dramatic elongation of microtubules toward the cortex, and active furrowing can be detected after a short latent period (Rappaport and Ebstein, 1965; Strickland *et al*., 2005). Although species and temperature dependent, the total time from anaphase onset to the initiation of furrowing in *L. pictus* has been measured to be ~7.5 min (Shuster and Burgess, 2002b). Mapping of contractile activity by compression revealed that myosin II activation coincides with the metaphase–anaphase transition (Figure 2), which considerably precedes the outgrowth of astral microtubules (Figure 6). Localization studies of microtubules and Ser19-phosphorylated light chain (Figure 3) as well as live cell imaging of EB1-decorated microtubules in the same species (Strickland *et al*., 2005) support the notion that at the metaphase–anaphase transition, the asters have yet to contact the cortex. Once the asters contact the cell cortex, Ser19 phosphorylation becomes restricted to the cleavage plane (Figure 3), and staining of phospho-Ser19 myosin regulatory light chain (PMLC) and myosin II (Figure 4) suggests that this zone of Ser19-phosphorylated regulatory light chain reflects local regulation of myosin II activity, and not simple redistribution of the motor. Indeed, recent mapping studies of RhoGTPase activity in sea urchin eggs revealed a microtubule-dependent zone of RhoA activity that precedes cleavage furrow formation (Bement *et al*., 2005), and the equatorial band of Ser19-MLC may be a reflection of local activation of RhoA.

Our findings that myosin II activation was independent of astral microtubules were further explored by altering microtubule polymerization or organization (Figure 7). Although nocodazole did not significantly alter myosin II activation, the dynamics of the contractile response was altered (Figure 7B′). In control cells (Figure 7, A and A′), an increase in cortical contractility during this transition was followed by a brief relaxation before furrowing. In contrast, nocodazole-treated cells (Figure 7C′) underwent a sharp increase in contractility that was sustained for up to 5 min without a subsequent relaxation phase. This raises the possibility that microtubules may partially suppress the global activation of contractility after anaphase onset. Similarly, whereas the presence of supernumery asters did not inhibit the global increase in contractility (Figure 7D′), the amplitude was dampened relative to controls. Together, these results suggest that although the initial myosin II activation is both independent of and occurs before cleavage plane determination, microtubules may play both positive and negative roles in confining contractility to the equatorial zone.

Signaling Pathways Regulating Myosin II Activation

Mapping of contractile activity by compression revealed that myosin II activation coincides with the metaphase–anaphase transition (Figure 2). This stands in contrast to earlier models for the timing of cytokinesis where myosin II activity was thought to be dependent on complete inactivation of cyclin-dependent kinase (Satterwhite *et al*., 1992; Satterwhite and Pollard, 1992). However, previous manipulation studies in sea urchin eggs (Shuster and Burgess, 1999) as well as in tissue culture cells (Rosenblatt *et al*., 2004) argue that myosin II activity may not be significantly suppressed during mitosis. Furthermore, mobilization of calcium early in mitosis resulted in a cortical contractile response (Figure 10), providing yet further evidence that myosin II is capable of responding to contractile signals in the presence of elevated cyclin-dependent kinase (CDK)1 activity. Studies of cylindrical sea urchin eggs suggested the presence of a molecular switch that signals the onset of cytokinesis and which is activated at the metaphase–anaphase transition (Shuster and Burgess, 2002b). It is possible that this switch identified in earlier experiments is related to the rise in cortical contractility observed in our compression assays.

There is strong evidence supporting the importance of ROCK as well as MLCK during cytokinesis (Poperechnaya *et al*., 2000; Matsumura *et al*., 2001; Chew *et al*., 2002; Matsumura, 2005). However, we find that although both signaling mechanisms are required for cytokinesis, they are required at different times. MLCK seems to be required for the global activation of myosin II at the metaphase–anaphase transition (Figure 8, C and D) as well as the ingression of the cleavage furrow (Figure 9), whereas inhibition of ROCK had no effect on the initial increase in myosin II activity, but it was required for furrow ingression (Figure 9). The notion that ROCK is required for myosin II regulation at later stages of cytokinesis is supported by time-lapse imaging of spherical ROCK-inhibited eggs, where furrows initiated but failed (our unpublished data). Together, these findings suggest that ROCK and MLCK are both required for cytokinesis but may serve different functional roles and may be activated at different times during mitotic progression. Indeed, studies in *Drosophila* indicate that although contractile rings can assemble and partially function in cells expressing nondegradable cyclin B3 (Parry and O'Farrell, 2001), Rho (and thus ROCK) function is not properly activated (Parry *et al*., 2003). Thus, Rho-dependent functions may lie downstream of the initial signal for cytokinesis, after microtubule contract with the cell cortex (Bement *et al*., 2005).

Global activation of contractility has been proposed in a number of models for cytokinesis (White and Borisy, 1983), but few mechanisms have been put forth to explain how a global activation of myosin II contributes to a process predicated on asymmetric distribution of force (cytokinesis). Schroeder proposed that a global activation of contractility primes the cortical cytoskeleton before cleavage plane determination and that astral microtubules disrupt this isometric contraction (Schroeder, 1981, 1990). Cytokinesis in *Dictyostelium* has been described as a two-phase process: an initial phase in which the cell transitions to a cylindrical shape and a second thinning phase during which the contractile ring constricts (Robinson *et al*., 2002; Reichl *et al*., 2005; Zhang and Robinson, 2005). It is during phase I of cytokinesis that the equatorial concentration of myosin II is at its greatest (Robinson *et al*., 2002), suggesting that the transition from a sphere to a cylinder requires the most force generation. It is possible that the principle role of MLCK is to provide contractile force during the initial steps in cell shape change (sphere to cylinder transition). This idea is supported by studies in isolated stress fibers, where MLCK is required for rapid contractile responses, and ROCK is required for slower, sustained contractions (Katoh *et al*., 2001). Last, myosin II regulation is spatially distinct in fibroblasts, with MLCK regulating peripheral contractility and ROCK regulating contractility in the cell center (Totsukawa *et al*., 2000; Totsukawa *et al*., 2004). Thus, it is not unreasonable to extrapolate such a model to sea urchin eggs, where MLCK regulates global (peripheral) contractile responses, and Rho-dependent kinases regulate contractility in response to spatial cues from the mitotic apparatus.

Reordering the Early Events of Cytokinesis

As discussed above, cytokinesis in animal cells is thought to include phases such as cleavage plane determination, contractile ring assembly, myosin II activation, ring constriction, disassembly of the contractile ring, and new membrane addition, followed by midbody formation. However, the finding that myosin II is activated before cleavage plane determination suggests that the above-mentioned events require some reorganization. Previous models for the timing of cytokinesis required that CDK1 activity drop before myosin II activation (Satterwhite *et al*., 1992). However, both our live cell analyses (Figures 1 and 2) as well as phospho-Ser19 staining (Figure 3) clearly demonstrate that myosin II activation occurs at the metaphase–anaphase transition, well before the other manifestations of mitotic exit. Myosin II contractility at the metaphase–anaphase transition both precedes and is independent of microtubules, thus placing activation of contractility before cleavage plane determination in the ordered phases of cytokinesis. In our revised model, the metaphase–anaphase transition triggers or is activated by a calcium transient (Groigno and Whitaker, 1998) that activates calmodulin and MLCK, thus resulting in myosin II activation and a global increase in cortical contractility. As CDK1 activity decreases and the astral microtubules elongate and contact the cortex, the global increase in contractility is transiently suppressed, resulting in a temporary decrease in contractility and relaxation of the cortex. Microtubule contacts with the cortical actin cytoskeleton directs the localized activation of Rho (Bement *et al*., 2005) and the recruitment of membrane microdomains (Ng *et al*., 2005), contributing not only to the organization of the ring but also to the maintenance of myosin II activation via ROCK and myosin phosphatase as the furrow ingresses. A detailed dissection of the relationship between mitotic exit and MLCK activation, similar to studies performed on cyclin destruction in *Drosophila* (Parry and O'Farrell, 2001; Echard and O'Farrell, 2003) as well as a functional evaluation of the apparent redundancy of myosin II-activating signals will provide better temporal resolution of this model.

ACKNOWLEDGMENTS

We thank David Burgess and Ray Rappaport for comments and suggestions and Rudolf Oldenbourg and Grant Harris for assistance with LC-PolScope imaging at the Marine Biological Laboratory. This work was supported by grants from the National Institute of General Medical Sciences (GM08136 and GM61222), and the Robert Day Allen and Baxter fellowships at the Marine Biological Laboratory.

REFERENCES

Bement, W. M., Benink, H. A., and von Dassow, G. (2005). A microtubule-dependent zone of active RhoA during cleavage plane specification. J. Cell Biol. *170*, 91–101.

Bresnick, A. R. (1999). Molecular mechanisms of nonmuscle myosin-II regulation. Curr. Opin. Cell Biol. *11*, 26–33.

Burgess, D. R., and Chang, F. (2005). Site selection for the cleavage furrow at cytokinesis. Trends Cell Biol. *15*, 156–162.

Burton, K., and Taylor, D. L. (1997). Traction forces of cytokinesis measured with optically modified elastic substrata. Nature *385*, 450–454.

Canman, J. C., and Bement, W. M. (1997). Microtubules suppress actomyosin-based cortical flow in *Xenopus* oocytes. J. Cell Sci. *110*, 1907–1917.

Chang, D. C., and Meng, C. (1995). A localized elevation of cytosolic free calcium is associated with cytokinesis in the zebrafish embryo. J. Cell Biol. *131*, 1539–1545.

Chew, T. L., Wolf, W. A., Gallagher, P. J., Matsumura, F., and Chisholm, R. L. (2002). A fluorescent resonant energy transfer-based biosensor reveals transient and regional myosin light chain kinase activation in lamella and cleavage furrows. J. Cell Biol. *156*, 543–553.

Cole, K. S. (1932). Surface forces of the *Arbacia* egg. J. Cell Comp. Physiol. *1*, 1–9.

Cole, K. S., and Michaelis, E. M. (1932). Surface forces of fertilized *Arbacia* eggs. J. Cell Comp. Physiol. *2*, 121–126.

Dechant, R., and Glotzer, M. (2003). Centrosome separation and central spindle assembly act in redundant pathways that regulate microtubule density and trigger cleavage furrow formation. Dev. Cell *4*, 333–344.

Dulyaninova, N. G., Malashkevich, V. N., Almo, S. C., and Bresnick, A. R. (2005). Regulation of myosin-IIA assembly and Mts1 binding by heavy chain phosphorylation. Biochemistry *44*, 6867–6876.

Echard, A., Hickson, G. R., Foley, E., and O'Farrell, P. H. (2004). Terminal cytokinesis events uncovered after an RNAi screen. Curr. Biol. *14*, 1685–1693.

Echard, A., and O'Farrell, P. H. (2003). The degradation of two mitotic cyclins contributes to the timing of cytokinesis. Curr. Biol. *13*, 373–383.

Egelhoff, T. T., Lee, R. J., and Spudich, J. A. (1993). Dictyostelium myosin heavy chain phosphorylation sites regulate myosin filament assembly and localization in vivo. Cell *75*, 363–371.

Eggert, U. S., Kiger, A. A., Richter, C., Perlman, Z. E., Perrimon, N., Mitchison, T. J., and Field, C. M. (2004). Parallel chemical genetic and genome-wide RNAi screens identify cytokinesis inhibitors and targets. PLoS Biol. *2*, e379

Fluck, R. A., Miller, A. L., and Jaffe, L. F. (1991). Slow calcium waves accompany cytokinesis in medaka fish eggs. J. Cell Biol. *115*, 1259–1265.

Girard, K. D., Chaney, C., Delannoy, M., Kuo, S. C., and Robinson, D. N. (2004). Dynacortin contributes to cortical viscoelasticity and helps define the shape changes of cytokinesis. EMBO J. *23*, 1536–1546.

Groigno, L., and Whitaker, M. (1998). An anaphase calcium signal controls chromosome disjunction in early sea urchin embryos. Cell *92*, 193–204.

Hiramoto, Y. (1963). Mechanical properties of sea urchin eggs. II. Changes in mechanical properties from fertilization to cleavage. Exp. Cell Res. *32*, 76–89.

Hiramoto, Y. (1970). Rheological properties of sea urchin eggs. Biorheology *6*, 201–234.

Hiramoto, Y. (ed.) (1990). Mechanical properties of the cortex before and during cleavage. Ann. NY Acad. Sci. *582*: 22–30.

Ikebe, M., Koretz, J., and Hartshorne, D. J. (1988). Effects of phosphorylation of light chain residues threonine 18 and serine 19 on the properties and conformation of smooth muscle myosin. J. Biol. Chem. *263*, 6432–6437.

Jordan, P., and Karess, R. (1997). Myosin light chain-activating phosphorylation sites are required for oogenesis in *Drosophila*. J. Cell Biol. *139*, 1805–1819.

Kallenbach, R. J. (1985). Ultrastructural analysis of the initiation and development of cytasters in sea-urchin eggs. J. Cell Sci. *73*, 261–278.

Kargacin, G. J., Ikebe, M., and Fay, F. S. (1990). Peptide modulators of myosin light chain kinase affect smooth muscle cell contraction. Am. J. Physiol. *259*, C315–C324.

Katoh, K., Kano, Y., Amano, M., Onishi, H., Kaibuchi, K., and Fujiwara, K. (2001). Rho-kinase–mediated contraction of isolated stress fibers. J. Cell Biol. *153*, 569–584.

Komatsu, S., Yano, T., Shibata, M., Tuft, R. A., and Ikebe, M. (2000). Effects of the regulatory light chain phosphorylation of myosin II on mitosis and cytokinesis of mammalian cells. J. Biol. Chem. *275*, 34512–34520.

Kovacs, M., Toth, J., Hetenyi, C., Malnasi-Csizmadia, A., and Sellers, J. R. (2004). Mechanism of blebbistatin inhibition of myosin II. J. Biol. Chem. *279*, 35557–35563.

Kuriyama, R., and Borisy, G. G. (1983). Cytasters induced within unfertilized sea-urchin eggs. J. Cell Sci. *61*, 175–189.

Larkin, K., and Danilchik, M. V. (1999). Microtubules are required for completion of cytokinesis in sea urchin eggs. Dev. Biol. *214*, 215–226.

Li, Z. H., Spektor, A., Varlamova, O., and Bresnick, A. R. (2003). Mts1 regulates the assembly of nonmuscle myosin-IIA. Biochemistry *42*, 14258–14266.

Lippincott, J., and Li, R. (1998). Sequential assembly of myosin II, an IQGAP-like protein, and filamentous actin to a ring structure involved in budding yeast cytokinesis. J. Cell Biol. *140*, 355–366.

Matsumura, F. (2005). Regulation of myosin II during cytokinesis in higher eukaryotes. Trends Cell Biol. *15*, 371–377.

Matsumura, F., Totsukawa, G., Yamakita, Y., and Yamashiro, S. (2001). Role of myosin light chain phosphorylation in the regulation of cytokinesis. Cell Struct. Funct. *26*, 639–644.

Matzke, R., Jacobson, K., and Radmacher, M. (2001). Direct, high-resolution measurement of furrow stiffening during division of adherent cells. Nat. Cell Biol. *3*, 607–610.

Miller, A. L., Fluck, R. A., McLaughlin, J. A., and Jaffe, L. F. (1993). Calcium buffer injections inhibit cytokinesis in *Xenopus* eggs. J. Cell Sci. *106*, 523–534.

Mitchison, J. M., and Swann, M. M. (1955). The mechanical properties of the cell surface: the sea urchin egg from fertilization to cleavage. J. Exp. Biol. *32*, 734–750.

Miyoshi, H., Satoh, S. K., Yamada, E., and Hamaguchi, Y. (2006). Temporal change in local forces and total force all over the surface of the sea urchin egg during cytokinesis. Cell Motil. Cytoskeleton *63*, 208–221.

Murakami, N., Chauhan, V. P., and Elzinga, M. (1998). Two nonmuscle myosin II heavy chain isoforms expressed in rabbit brains: filament forming properties, the effects of phosphorylation by protein kinase C and casein kinase II, and location of the phosphorylation sites. Biochemistry *37*, 1989–2003.

Murakami, N., Kotula, L., and Hwang, Y. W. (2000). Two distinct mechanisms for regulation of nonmuscle myosin assembly via the heavy chain: phosphorylation for MIIB and mts 1 binding for MIIA. Biochemistry *39*, 11441–11451.

Muto, A., Kume, S., Inoue, T., Okano, H., and Mikoshiba, K. (1996). Calcium waves along the cleavage furrows in cleavage-stage *Xenopus* embryos and its inhibition by heparin. J. Cell Biol. *135*, 181–190.

Naim, V., Imarisio, S., Di Cunto, F., Gatti, M., and Bonaccorsi, S. (2004). Drosophila citron kinase is required for the final steps of cytokinesis. Mol. Biol. Cell *15*, 5053–5063.

Ng, M. M., Chang, F., and Burgess, D. R. (2005). Movement of membrane domains and requirement of membrane signaling molecules for cytokinesis. Dev. Cell *9*, 781–790.

O'Halloran, T. J., and Spudich, J. A. (1990). Genetically engineered truncated myosin in Dictyostelium: the carboxyl-terminal regulatory domain is not required for the developmental cycle. Proc. Natl. Acad. Sci. USA *87*, 8110–8114.

Ohtsubo, M., and Hiramoto, Y. (1985). Regional differences in mechanical properties of the cell surface in dividing echinoderm eggs. Dev. Growth Differ. *27*, 371–383.

Oldenbourg, R., and Mei, G. (1995). New polarized light microscope with precision universal compensator. J. Microsc. *180*, 140–147.

Parry, D. H., Hickson, G. R., and O'Farrell, P. H. (2003). Cyclin B destruction triggers changes in kinetochore behavior essential for successful anaphase. Curr. Biol. *13*, 647–653.

Parry, D. H., and O'Farrell, P. H. (2001). The schedule of destruction of three mitotic cyclins can dictate the timing of events during exit from mitosis. Curr. Biol. *11*, 671–683.

Piekny, A., Werner, M., and Glotzer, M. (2005). Cytokinesis: welcome to the Rho zone. Trends Cell Biol. *15*, 651–658.

Poperechnaya, A., Varlamova, O., Lin, P. J., Stull, J. T., and Bresnick, A. R. (2000). Localization and activity of myosin light chain kinase isoforms during the cell cycle. J. Cell Biol. *151*, 697–708.

Rappaport, R. (1996). Cytokinesis in Animal Cells, Cambridge, United Kingdom: Cambridge University Press.

Rappaport, R., and Ebstein, R. P. (1965). Duration of stimulus and latent periods preceding furrow formation in sand dollar eggs. J. Exp. Zool. *158*, 373–382.

Rappaport, R., and Rappaport, B. N. (1993). Duration of division-related events in cleaving sand dollar eggs. Dev. Biol. *158*, 265–273.

Reichl, E. M., Effler, J. C., and Robinson, D. N. (2005). The stress and strain of cytokinesis. Trends Cell Biol. *15*, 200–206.

Robinson, D. N., Cavet, G., Warrick, H. M., and Spudich, J. A. (2002). Quantitation of the distribution and flux of myosin-II during cytokinesis. BMC Cell Biol. *3*, 4

Robinson, D. N., and Spudich, J. A. (2000). Dynacortin, a genetic link between equatorial contractility and global shape control discovered by library complementation of a *Dictyostelium discoideum* cytokinesis mutant. J. Cell Biol. *150*, 823–838.

Rosenblatt, J., Cramer, L. P., Baum, B., and McGee, K. M. (2004). Myosin II-dependent cortical movement is required for centrosome separation and positioning during mitotic spindle assembly. Cell *117*, 361–372.

Sabry, J. H., Moores, S. L., Ryan, S., Zang, J. H., and Spudich, J. A. (1997). Myosin heavy chain phosphorylation sites regulate myosin localization during cytokinesis in live cells. Mol. Biol. Cell *8*, 2605–2615.

Satterwhite, L. L., Lohka, M. J., Wilson, K. L., Scherson, T. Y., Cisek, L. J., Corden, J. L., and Pollard, T. D. (1992). Phosphorylation of myosin-ii regulatory light chain by cyclin-p34cdc 2, a mechanism for the timing of cytokinesis. J. Cell Biol. *118*, 595–605.

Satterwhite, L. L., and Pollard, T. D. (1992). Cytokinesis. Curr. Opin. Cell Biol. *4*, 43–52.

Saul, D., Fabian, L., Forer, A., and Brill, J. A. (2004). Continuous phosphatidylinositol metabolism is required for cleavage of crane fly spermatocytes. J. Cell Sci. *117*, 3887–3896.

Scholey, J. M., Taylor, K. A., and Kendrick-Jones, J. (1980). Regulation of non-muscle myosin assembly by calmodulin-dependent light chain kinase. Nature *287*, 233–235.

Schroeder, T. E. (1972). The contractile ring II. determining its brief existence, volumetric changes, and vital role in cleaving *Arbacia* eggs. J. Cell Biol. *53*, 419–434.

Schroeder, T. E. (1981). The origin of cleavage forces in dividing eggs: a mechanism in two steps. Exp. Cell Res. *134*, 231–240.

Schroeder, T. E. (1990). The contractile ring and furrowing in dividing cells. Ann. NY Acad. Sci. *582*, 78–87.

Shu, S., Liu, X., and Korn, E. D. (2005). Blebbistatin and blebbistatin-inactivated myosin II inhibit myosin II-independent processes in *Dictyostelium*. Proc. Natl. Acad. Sci. USA *102*, 1472–1477.

Shuster, C. B., and Burgess, D. R. (1999). Parameters that specify the timing of cytokinesis. J. Cell Biol. *146*, 981–992.

Shuster, C. B., and Burgess, D. R. (2002a). Targeted new membrane addition in the cleavage furrow is a late, separate event in cytokinesis. Proc. Natl. Acad. Sci. USA *99*, 3633–3638.

Shuster, C. B., and Burgess, D. R. (2002b). Transitions regulating the timing of cytokinesis in embryonic cells. Curr. Biol. *12*, 854–858.

Simerly, C., Nowak, G., de Lanerolle, P., and Schatten, G. (1998). Differential expression and functions of cortical myosin IIA and IIB isotypes during meiotic maturation, fertilization, and mitosis in mouse oocytes and embryos. Mol. Biol. Cell *9*, 2509–2525.

Skop, A. R., Liu, H., Yates, J., 3rd, Meyer, B. J., and Heald, R. (2004). Dissection of the mammalian midbody proteome reveals conserved cytokinesis mechanisms. Science *305*, 61–66.

Sluder, G. (1976). Experimental manipulation of the amount of tubulin available for assembly into the spindle of dividing sea urchin eggs. J. Cell Biol. *70*, 75–85.

Sluder, G. (1979). Role of spindle microtubules in the control of cell cycle timing. J. Cell Biol. *80*, 674–691.

Sluder, G., Miller, F. J., and Hinchcliffe, E. H. (1999). Using sea urchin gametes for the study of mitosis. Methods Cell Biol. *61*, 439–472.

Sluder, G., Thompson, E., Miller, F., Hayes, J., and Rieder, C. (1997). The checkpoint control for anaphase onset does not monitor excess numbers of spindle poles or bipolar spindle symmetry. J. Cell Sci. *110*, 421–429.

Stack, C., Lucero, A. J., and Shuster, C. B. (2006). Calcium-responsive contractility during fertilization in sea urchin eggs. Dev. Dyn. *235*, 1042–1052.

Straight, A. F., Cheung, A., Limouze, J., Chen, I., Westwood, N. J., Sellers, J. R., and Mitchison, T. J. (2003). Dissecting Temporal and Spatial Control of Cytokinesis with a Myosin II Inhibitor. Science *299*, 1743–1747.

Strickland, L. I., Donnelly, E. J., and Burgess, D. R. (2005). Induction of cytokinesis is independent of precisely regulated microtubule dynamics. Mol. Biol. Cell.

Totsukawa, G., Wu, Y., Sasaki, Y., Hartshorne, D. J., Yamakita, Y., Yamashiro, S., and Matsumura, F. (2004). Distinct roles of MLCK and ROCK in the regulation of membrane protrusions and focal adhesion dynamics during cell migration of fibroblasts. J. Cell Biol. *164*, 427–439.

Totsukawa, G., Yamakita, Y., Yamashiro, S., Hartshorne, D. J., Sasaki, Y., and Matsumura, F. (2000). Distinct roles of ROCK (Rho-kinase) and MLCK in spatial regulation of MLC phosphorylation for assembly of stress fibers and focal adhesions in 3T3 fibroblasts. J. Cell Biol. *150*, 797–806.

Usui, N., and Yoneda, M. (1982). Ultrstructural basis of the tension increase in sea-urchin eggs prior to cytokinesis. Dev. Growth Differ. *24*, 453–465.

Wang, Y. L. (2005). The mechanism of cortical ingression during early cytokinesis: thinking beyond the contractile ring hypothesis. Trends Cell Biol. *15*, 581–588.

Webb, S. E., Lee, K. W., Karplus, E., and Miller, A. L. (1997). Localized calcium transients accompany furrow positioning, propagation, and deepening during the early cleavage period of zebrafish embryos. Dev. Biol. *192*, 78–92.

Wheatley, S. P., and Wang, Y. L. (1996). Midzone microtubule bundles are continuously required for cytokinesis in cultured epithelial cells. J. Cell Biol. *135*, 981–989.

White, J. G., and Borisy, G. G. (1983). On the mechanisms of cytokinesis in animal cells. J. Theor. Biol. *101*, 289–316.

Wilson, E. B. (1928). The Cell in Development and Heredity, New York: The MacMillan Company.

Wong, G. K., Allen, P. G., and Begg, D. A. (1997). Dynamics of filamentous actin organization in the sea urchin egg cortex during early cleavage divisions: implications for the mechanism of cytokinesis. Cell Motil. Cytoskeleton *36*, 30–42.

Wong, R., Hadjiyanni, I., Wei, H. C., Polevoy, G., McBride, R., Sem, K. P., and Brill, J. A. (2005). PIP2 hydrolysis and calcium release are required for cytokinesis in *Drosophila* spermatocytes. Curr. Biol. *15*, 1401–1406.

Wu, J. Q., Kuhn, J. R., Kovar, D. R., and Pollard, T. D. (2003). Spatial and temporal pathway for assembly and constriction of the contractile ring in fission yeast cytokinesis. Dev. Cell *5*, 723–734.

Wu, J. Q., and Pollard, T. D. (2005). Counting cytokinesis proteins globally and locally in fission yeast. Science *310*, 310–314.

Yoneda, A. (1964). Tension at the surface of sea urchin egg: a critical examination of Coles's experiment. J. Exp. Biol. *41*, 893–906.

Yoneda, M. (1986). The compression method for determining the surface force. Methods Cell Biol. *27*, 421–434.

Yoneda, M., and Dan, K. (1972). Tension at the surface of the dividing sea-urchin egg. J. Exp. Biol. *57*, 575–587.

Yoneda, M., Ikeda, M., and Washitani, S. (1978). Periodic change in the tension at the surface of activated non-nucleated fragments of the sea-urchin eggs. Dev. Growth Differ. *20*, 329–336.

Yoneda, M., and Schroeder, T. E. (1984). Cell cycle timing in colchicine-treated sea urchin eggs: persistent coordination between the nuclear cycles and the rhythm of cortical stiffness. J. Exp. Zool. *231*, 385–391.

Yumura, S. (2001). Myosin II dynamics and cortical flow during contractile ring formation in *Dictyostelium* cells. J. Cell Biol. *154*, 137–146.

Yumura, S., and Uyeda, T. Q. (1997). Transport of myosin II to the equatorial region without its own motor activity in mitotic *Dictyostelium* cells. Mol. Biol. Cell *8*, 2089–2099.

Yumura, S., Yoshida, M., Betapudi, V., Licate, L. S., Iwadate, Y., Nagasaki, A., Uyeda, T. Q., and Egelhoff, T. T. (2005). Multiple myosin ii heavy chain kinases: roles in filament assembly control and proper cytokinesis in *Dictyostelium*. Mol. Biol. Cell.

Zang, J. H., and Spudich, J. A. (1998). Myosin II localization during cytokinesis occurs by a mechanism that does not require its motor domain. Proc. Natl. Acad. Sci. USA *95*, 13652–13657.

Zhang, W., and Robinson, D. N. (2005). Balance of actively generated contractile and resistive forces controls cytokinesis dynamics. Proc. Natl. Acad. Sci. USA *102*, 7186–7191.